The Journal of Experimental Biology 212, 1351-1364
Published by The Company of Biologists 2009
doi:10.1242/jeb.022566

Waveform generation in the weakly electric fish *Gymnotus coropinae* (Hoedeman): the electric organ and the electric organ discharge

María E. Castelló, Alejo Rodríguez-Cattáneo, Pedro A. Aguilera, Leticia Iribarne, Ana Carolina Pereira and Ángel A. Caputi*

Departamento de Neurociencias Integrativas y Computacionales, Instituto de Investigaciones Biológicas Clemente Estable, Avenida Italia 3318, CP 11600, Montevideo, Uruguay

*Author for correspondence (e-mail: angel@iibce.edu.uy)

Accepted 5 February 2009

SUMMARY

This article deals with the electric organ and its discharge in *Gymnotus coropinae,* a representative species of one of the three main clades of the genus. Three regions with bilateral symmetry are described: (1) subopercular (medial and lateral columns of complex shaped electrocytes); (2) abdominal (medial and lateral columns of cuboidal and fusiform electrocytes); and (3) main [four columns, one dorso-lateral (containing fusiform electrocytes) and three medial (containing cuboidal electrocytes)]. Subopercular electrocytes are all caudally innervated whereas two of the medial subopercular ones are also rostrally innervated. Fusiform electrocytes are medially innervated at the abdominal portion, and at their rostral and caudal poles at the main portion. Cuboidal electrocytes are always caudally innervated. The subopercular portion generates a slow head-negative wave (V_{1r}) followed by a head-positive spike (V_{3r}). The abdominal and main portions generate a fast tetra-phasic complex (V_{2345ct}). Since subopercular components prevail in the near field and the rest in the far field, time coincidence of V_{3r} with V_2 leads to different waveforms depending on the position of the receiver. This confirms the splitting hypothesis of communication and exploration channels based on the different timing, frequency band and reach of the regional waveforms. The following hypothesis is compatible with the observed anatomo-functional organization: V_{1r} corresponds to the rostral activation of medial subopercular electrocytes and V_{3r} to the caudal activation of all subopercular electrocytes; V_2, and part of V_{3ct}, corresponds to the successive activation of the rostral and caudal poles of dorso-lateral fusiform electrocytes; and V_{345ct} is initiated in the caudal face of cuboidal electrocytes by synaptic activation (V_{3ct}) and it is completed (V_{45ct}) by the successive activation of rostral and caudal faces by the action currents evoked in the opposite face.

Supplementary material available online at http://jeb.biologists.org/cgi/content/full/212/9/1351/DC1

Key words: fixed motor pattern, electrocyte, signal carrier, three-dimensional reconstruction, evolution.

INTRODUCTION

Electric fish have an electrogenic system that generates a complex and spatio-temporally stereotyped electric field (Lissmann, 1951) (reviewed by Caputi et al., 2005). This field is used by the fish as a carrier of electric signals for active sensing of the environment (Lissmann and Machin, 1958) and communicating with other electric fish (Mohres, 1957). The signal used for active sensing of the environment is the modulation of the fish's self-generated field imposed by any electric heterogeneity in the surrounding water, and social communication is based on the modulation of the rate or waveform of the emitted discharge.

In the case of active exploration, the presence of objects modifies the self-generated electric field, changing the transcutaneous pattern of currents on the skin of the emitting fish. This pattern forms an electric image of the environment, from which some features, depending on the shape, distance and conductivity of nearby objects, can be used as information (Caputi and Budelli, 2006).

In the case of electro-communication, signals received by one fish are generated by the active emissions of another fish. The amplitude, waveform and repetition rate of the emitted EODs can be controlled in different ways in order to encode different kinds of messages (Hopkins and Bass, 1981; Hopkins et al., 1990; Silva et al., 2002; Stoddard, 2006).

Electric images thus generated at the skin surface are sensed by a mosaic of electroreceptors distributed non-homogeneously over the fish body. This mosaic was considered as an 'electrosensory retina' by Lissmann (Lissmann, 1958). An electrosensory fovea has been described in the perioral region of this 'retina', in *Gymnotus n. sp. omari*, a member of one of the most wide-spread genera of South American pulse gymnotids (Castelló et al., 2000). More recently a similar organization was described in *Gnathonemus petersii*, an African weakly discharging electric fish having convergent evolution (von der Emde and Schwartz, 2002; Bacelo et al., 2008; Pusch et al., 2008).

Electroreceptors are precisely tuned to the temporal features of the self-generated electric organ discharge (sEOD) and to the EODs produced by individuals of the same genus (Hopkins, 1976; Watson and Bastian, 1979). The species specificity of the EOD waveform endows each species with semi-private channels for their electric sense, which may play a role in individual and species recognition, or in avoiding predators (Hopkins and Bass, 1981; McGregor and Westby, 1992; Stoddard, 1999).

The variety of species-specific EOD waveforms provides a functional signature for species classification and suggests that the process of speciation is related to the evolution of the electrogenic system (Albert and Crampton, 2005). In consequence, the study of

the diversity of electric organs (EOs) and EOD waveforms may be a first step in identifying the commonalities and differences of the electrogenic mechanisms and the evolution of their traits (Rodríguez-Cattáneo et al., 2008).

This article deals with the EO and EOD of *Gymnotus coropinae* (Hoedeman, 1962; Crampton and Albert, 2003). We described the pattern of electromotive force, the EOD-associated electric field and the anatomical organization of the electrogenic tissue. A brief background is provided to familiarize the reader with the electrogenic system of the taxonomic group to which *G. coropinae* belongs.

In pulse gymnotids, the EOD generates a field in which the temporal waveform consists of a succession of three to five waves. Their relative amplitudes depend on the recording site with respect to the fish body. The EO is long, stretching over 90% of the fish's length. It is heterogeneous, generating discharges with different waveforms and amplitudes at different regions of the fish body. As the fish body is tapered, the different regions impose a different internal load on the EOD. The power dissipated externally thus depends on the ratio of internal and external resistances, which differs along the length of the fish. This means that the form of the field differs at different points in space relative to the fish (for reviews, see Bennett, 1971; Caputi, 1999; Caputi et al., 2005).

Near the fish the waveform is site-dependent and 'illuminates' objects sufficiently for electrolocation, giving information about size, shape, electrical properties and position relative to the fish's body in the 'near field'. Further away, the field is weaker and the waveform is much less dependent on site relative to the fish's body. In this 'far field' the EOD cannot serve for analysis of the environment but serves as a carrier for communication signals. Thus, comparison of 'near fields' and 'far fields' gives information about both the spatial origin of their components and their functional role in electrolocation.

The EO is composed of a series of electrogenic units, the electrocytes, whose activity is coordinated by the nervous system. This gives an additional factor contributing to the complexity of the electric field, which results from the spatio-temporal summation of the responses of different types of electrocytes, acting on different loads depending on their location along the EO.

It is interesting to note that long before the functional roles of the EO were established, when discussing the difficulties of the theory of natural selection, Darwin (Darwin, 1866) wrote: *"But when we look at the subject more closely, we find in several fishes provided with electric organs that they differ in construction, as in the arrangement of the plates, and according to Pacini, in the process by which the electricity is excited – and lastly, in being supplied with nerves proceeding from different sources, and this is perhaps the most of all the differences"*. Modern studies coming after the discovery of electroreception have confirmed this assertion, and have identified the following principal features of EOs that determine EOD waveform and give the species identity: (1) the pattern of electrocyte innervation, (2) electrocyte shape and intrinsic properties, and (3) electrocyte density distribution.

Bennett and Grundfest (Bennett and Grundfest, 1959) showed the importance of the innervation pattern in determining the polarity of the wave components in *Gymnotus carapo*. These observations were confirmed by anatomical studies showing the presence of separate innervations of the rostral and caudal faces of some electrocytes, implying that the generation of each wave component is a subcellular process related to the orientation of current flow through the neighboring tissue (Szabo, 1961; Trujillo-Cenóz et al., 1984; Trujillo-Cenóz and Echagüe, 1989; Caputi et al., 1994). The electrocytes are arranged in series in longitudinal tubes. This causes a dominant rostro-caudal flow of current through the muscle tissue surrounding the EO in such way that each region of the body, containing a portion of the EO, behaves as an electric source with low internal resistance. The regional waveform results from the spatio-temporal summation of postsynaptic and action currents generated by different electrogenic membranes, activated in a sequence precisely coordinated by the nervous system. A clear example of this process was illustrated by Bennett and Grundfest (Bennett and Grundfest, 1959), and by Lorenzo et al. (Lorenzo et al., 1988), who showed that the activation of two different nerves projecting, respectively, to the rostral and caudal faces of the same electrocyte, reproduced the regional waveform when stimuli were applied with the proper delay.

Another determinant of local waveform is electrocyte responsiveness. Depending on membrane responsiveness, some wave components result from a direct effect of the synaptic activation of a membrane patch and others result from the propagation of the action potential from innervated to non-innervated regions of the same electrocyte (Bennet and Grundfest, 1959; Caputi et al., 1989; Caputi et al., 1994; Caputi et al., 1998). This propagation depends on electrocyte size, shape and membrane properties (Caputi et al., 1989; Caputi et al., 1994; Caputi et al., 1998; Sierra, 2007; Rodríguez-Cattáneo et al., 2008). Action potentials originated on the innervated faces of small electrocytes are more likely to activate the opposite face, thus generating a biphasic complex, whereas large electrocytes are more likely to contribute to monophasic components of the EOD.

The third factor, electrocyte distribution, is also important for setting the differences between regional waveforms. Electrocytes may be classified into types according to the number of independent membrane patches that are innervated (singly, doubly, etc). Each type of electrocyte occupies a different domain along the EO, and electrocyte density increases from head to tail in most species [*G. omari* (Trujillo-Cenóz and Echagüe, 1989); and other *Gymnotus* (M.E.C., A.R.-C., P.A.A., L.I., A.C.P. and A.A.C., unpublished observations), *Rhamphichthys rostratus* (Caputi et al., 1994)]. This causes regional differences in waveform. In addition, electrocyte density increases exponentially from head to tail, causing a similar increase in EOD amplitude (Caputi et al., 1989; Pereira et al., 2007). Although in most species the larger variety of electrocyte types occurs in the rostral and intermediate regions of the fish body, the tail region is generally similar across species, consisting of a dense population of caudally innervated electrocytes. This difference in electrocyte distribution, as well as the difference in excitability of rostral membranes, causes a variety of wave components that can be identified not only by their timing but also by their shape and spatial origin along the fish body (Caputi et al., 1989; Caputi et al., 1994; Rodríguez-Cattáneo et al., 2008). As a consequence, the rostral and intermediate regions generate complex waveforms resulting from the activation of different membrane patches in different electrocyte types by different nerves. Conversely, the tail regions generate complex waveforms resulting from similar complex responses of a single type of electrocyte to a single synaptic activation of its caudal face. Depending on electrocyte excitability, biphasic EOD (propagation of the action potential from caudal to rostral faces), or triphasic EOD (propagation of the action potential from caudal to rostral faces, and back to caudal faces) occurs (Rodríguez-Cattáneo et al., 2008).

Finally, the tapered shape and low internal resistance of the fish body causes a rostral funneling of the caudally generated currents. This phenomenon increases the relative length of the equivalent source for caudally generated components. Thus, rostrally generated components mainly flow around the head and have a shorter reach, 'illuminating' the region of space where objects generate foveal

images and thus are involved in active electrolocation. Conversely, caudally generated components tend to flow between rostral and caudal regions, and have a larger reach. These post-effector–pre-receptor mechanisms split the electrosensory carrier into two sub-components differentiated by their waveform and reach: the 'near field' for electrical exploration of the surroundings (mainly stimulating the foveal region), and the 'far field' for electrocommunication (Castelló et al., 2000; Aguilera et al., 2001).

Our findings on the EO and the EOD of *G. coropinae* reported here confirm the previously described general organization of the EO and also show the presence of a cephalic portion of the EO. This portion is responsible for the local field that is probably involved in active electrolocation. This regional discharge, which has the lowest frequency components, precedes the caudal discharge that has a higher frequency band spectrum. We can conclude that in this species, rostrally and caudally generated components not only differ in their reach (because of fish body post-effector filtering), but also on their timing and frequency components. From the structure of the EO and its innervation pattern, we hypothesize a pattern of activation that explains the recorded EOD.

MATERIALS AND METHODS

Twelve, sexually undifferentiated, *Gymnotus coropinae* [captured by W. G. R. Crampton in Surinam, and also used in the study by Rodríguez-Cattáneo et al. (Rodríguez-Cattáneo et al., 2008)] were employed for the detailed analysis of the EO anatomy, electrocyte innervation pattern, electromotive force and EOD-associated electric field. All potentially harmful procedures were conducted under anesthesia, following IIBCE's regulations for the use of experimental animals, the guidelines of the Universidad de la República (CHEA), and the Society for Neuroscience.

Anatomy and innervation of the electrogenic tissue

Fish were fixed under deep anesthesia (MS-222, 250 mg l^{-1}, up to apnea). The structure of the EO and the distribution of the thin nerve bundles, as well as the arrangement of the electromotor nerve terminals on the electrocytes' surfaces were studied using silver impregnated tissue samples. For this purpose, after a combined fixation and decalcification step [De Castro's formulae (Ramón y Cajal and De Castro, 1933)] the whole head or its inferior half including the jaw, the abdominal wall, and four to five consecutive portions of the middle part of the fish body and tail, were impregnated with silver ($AgNO_3$, 1.5%, for 7 days at 37°C) and subsequently reduced in formaldehyde-hydroquinone. Tissues were embedded in a soft mixture of epoxy resin and cut into serial sections (30 μm thick).

The head portion of the EO was serially sectioned either in frontal (N=1), parasagittal (N=1), or horizontal (N=2) planes. The abdominal wall containing the EO was removed as a whole, fixed attached to a plane surface, and studied in serial horizontal sections. The organization and innervation of the rest of the EO was studied using a series of frontal and parasagittal sections obtained from three well impregnated specimens. Frontal sections representative of the different portions of the fish were used for the visualization of the gross anatomy of the fish body, and the relative size and position of the EO.

Sections were examined under the light microscope and digital images were acquired using different optical and CCD resolutions. Computational three-dimensional (3-D) reconstructions of the EO, its innervation, and some of the topographically related structures were performed using BioVis3D© (www.biovis3D.com). This required the combined observation of the series of low power images loaded into the 3-D reconstructions with the concomitant examination of the sections under high resolution objectives.

Measurements and representation of EOD-associated electric fields

Electric fields produced by the EOD were recorded with the fish resting in a pen made of nylon netting at the center of a plastic tank (48 cm×28 cm filled with water up to 4 cm depth (conductivity: 30 μS cm^{-1}; temperature: 24°C). The back and forth movements of the fish were minimized using stitches to adjust the net to the shape of the body.

We used two recording procedures: (1) the longitudinal head to tail EOD (htEOD) fields, recorded using two silver/silver chloride electrodes, each placed on the middle line of the tank at different distances (steps of 4 cm up to the limits of the tank), one in front of the head and the other behind the tail; (2) the near-field recordings (Local EOD, LEOD) were measured using a specially designed LEOD probe placed close to the skin of the fish at different points along its body. The latter technique (for details, see Aguilera et al., 2001; Rodríguez-Cattáneo et al., 2008) was used to record local potential gradients equivalent to the orthogonal components of the local electric field vector at that point. The LEOD probe was constructed from three wires, insulated except at their tips. Active electrodes were oriented along horizontal orthogonal axes (perpendicular and parallel to the main body axis) intersected at the point where the reference was placed (facing the point on the skin under investigation). The tip of the active electrodes was 2.5 mm from the reference electrode. We carried out two types of experiments. First we recorded LEODs of the head region at equally spaced points (2 mm steps) along a parasagittal line passing 2 mm from the nearest point on the fish skin surface at the middle of the fish height. Second, we recorded the field at equally spaced points (1 cm steps) along five parasagittal lines separated, respectively, 1, 2, 3, 4 or 5 cm from the fish's nearest point. 'Vector plots' were constructed for every sampled time of the EOD using the two simultaneous orthogonal fields obtained at each and every recording position.

The voltage differences between each of the active electrodes and the common reference electrode of the LEOD probe, and between the two electrodes recording the htEOD were measured using a high-input impedance, high-gain, differential amplifier (10–20 kHz band-pass filter). Recorded waveforms were sampled (25–50 kHz, depending on the number of channels recorded, 16 bits) and displayed on a computer screen. Voltage measurements were considered to be proportional to the voltage gradient along the orthogonal axes and, therefore, to the horizontal components of the LEOD. Using these data we performed a source–sink analysis that was complementary to the measurements made in the air gap system.

Measurements of the source parameters

To evaluate the spatio-temporal pattern of equivalent electromotive force (EMF) for the fish body we used the air-gap technique (Cox and Coates, 1938; Bell et al., 1976; Caputi et al., 1989), which consists of the simultaneous recording of the voltage drop generated by different portions of the fish's body when isolated in air. In the simplest version this procedure estimates holistically the EMF and the internal resistance of the fish's body (R_i) by recording the drop of voltage (V) across a variable loading resistor connected to the head and to the tail in such a way that all the external current (I) generated by the fish body is funneled through the load.

The EMF is then calculated as the ordinate intersection of the function relating V and I:

$$V = EMF - R_i \times I ,$$

where R_i in series with the EMF corresponds to the equivalent resistance resultant from the parallel array of the resistances of

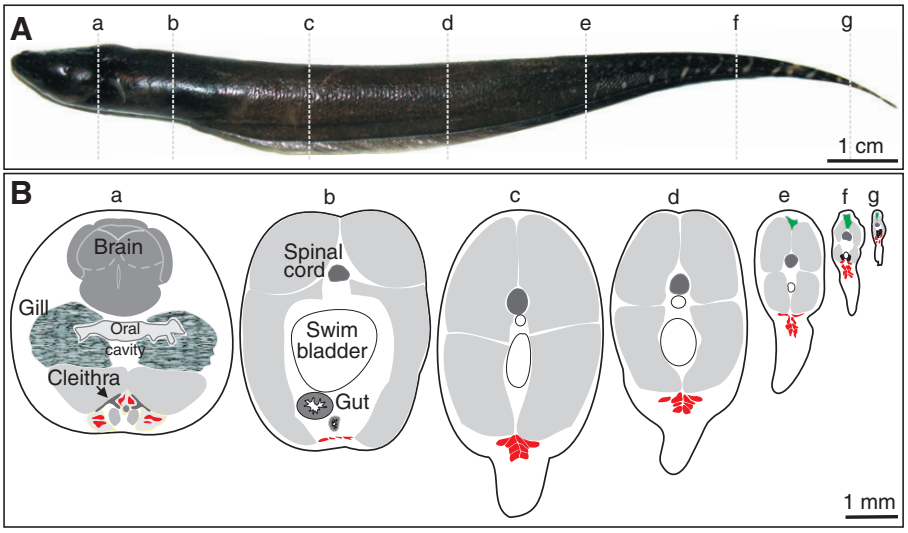

Fig. 1. Gross anatomy of the electric organ as observed in frontal sections of the fish body. (A) Photograph of a specimen of *G. coropinae* in which the vertical lines (a to g) indicate positions of sections shown in the diagrams in B. (B) In each diagram some non-electrogenic structures are shown in different gray tones, and the tubes that contain the electrogenic tissue are shown in red. Three portions of the EO can be clearly distinguished: (1) subopercular, in which the EO consists of a medial and a lateral columns (section a); (2) abdominal, in which the EO is included in the abdominal wall (section b); and (3) main, along the rest of the body in which the EO occupies the region between the ventral muscles and the fin (sections c to g). A relatively large posterior electromotor nerve is present in the caudal region (in black in f and g) and a jelly-like material between the dorsal muscles, similar to that present between the electrocytes in the EO tubes (in green in e to g).

electrogenic and non-electrogenic tissues (Caputi et al., 1989). However, in the case of the wave components generated by a non-innervated face, the electromotive force may be dependent on the propagation of action potentials from the innervated face (Bell et al., 1976; Caputi et al., 1998). Since action potential propagation is load dependent, the voltage *versus* current plot could yield a non linear relationship.

For the multiple air gap exploration of the regional EMFs (Caputi et al., 1993), fish were suspended in the air using a custom made apparatus that holds the fish as in a grill. The apparatus consists of

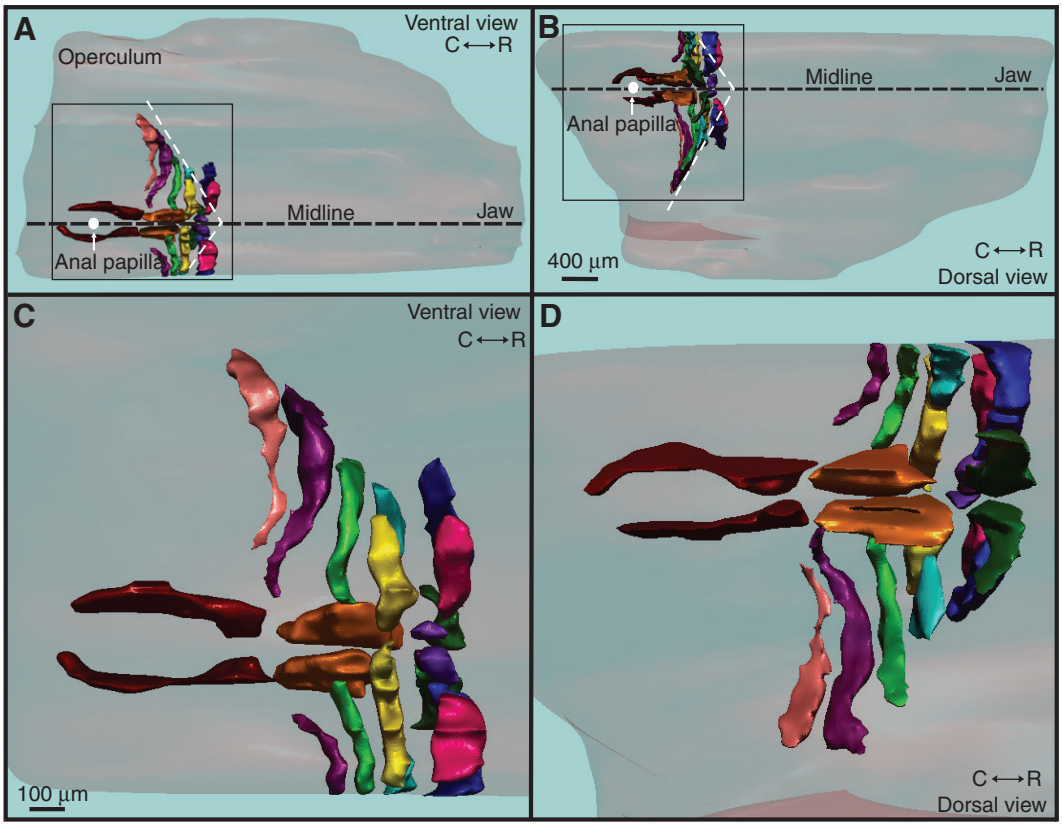

Fig. 2. Computer aided 3-D reconstruction of the subopercular portion of the EO based on serial parasagittal sections of the ventral half of the head impregnated according to the procedure of Cajal and De Castro. Ventral (A) and dorsal (B) views of a 3-D reconstruction of the ventral half of the head (cleared profile) to show the relative position of the subopercular portion of the EO. The position of the cleithrum is indicated in A and B by the dashed line. (C,D) Same views as in A and B with higher digital zoom to show the arrangement of electrocytes of the subopercular EO. At each side of the midline, two columns of electrocytes are evident. One medial, containing two rostro-caudally elongated electrocytes (dark and light brown), one elongated in the dorso-ventral axis (dark green), and a cuboidal electrocyte beneath it (dark blue). The axis of the lateral column of electrocytes follows an oblique course. It consists of seven ribbon-like electrocytes with their main dimension in the frontal plane (pink, violet, light green, cyan, yellow, blue and magenta).

seven parallel wires perpendicular to the main axis of the body, placed in contact with the skin, one at each extreme of the fish and the others at the limits of the explored regions. Six regions of the fish body were considered: one region comprising the head and the abdomen (two-sevenths of the fish length) and five consecutive caudal regions (each comprising one seventh of the fish length). Voltages recorded between pairs of wires were amplified to reach adequate amplitude for similar quantization (always larger than 8 bits) and sampled at 25 kHz. In the air gap condition, there was no load, so voltage recordings were considered good estimators of the equivalent electromotive forces generated by different portions of the fish's body when the electric organ is activated. However, this was not the case for all wave components (see Results).

RESULTS

The electric organ

The electrogenic tissue occupies a small fraction of the cross-sectional area, mainly located in the ventral region of the fish body, from the subopercular region of the head to the tip of the tail. This tissue is organized as a single EO consisting of parallel columns or tubes of different length. These tubes are delimited by connective tissue, and divided into compartments by thin perpendicular septa (Couceiro and De Almeida, 1961). Each compartment contains a syncytial multinucleated unit, called an electrocyte, usually shorter than the compartment; the rest of the compartment contains a jelly tissue through which the electromotor axons travel. A similar jelly tissue was found in the dorsal region of the most caudal quarter of the fish body, above the spine and between the dorsal muscle masses. We did not find electrocytes in this tissue.

We defined three different types of electrocytes according to their shapes: cuboidal, ribbon like and fusiform. These vary in size and innervation patterns depending on their location along the EO. Three distinct portions of the EO were distinguished taking into account the general organization, and the types and densities of the electrocytes: subopercular, abdominal, and main (Fig. 1).

The subopercular portion of the electric organ

The subopercular portion occupies the ventro-medial and caudal portion of the head, rostral to the anal papilla, ventral to the heart, and partly encased by the cleithra bones (Fig. 1B section a, Fig. 2). Cleithra are paired, crescent shaped, flat bones that are the main supports of the shoulder girdle. They are just visible under the skin, on either side of the head immediately behind the gills; a connective sheath spans between them and the opercular bones. Computational 3-D reconstructions of this portion allowed us to elucidate its intricate structural organization (Figs 2 and 3; see also Movie 1 in supplementary material). This portion of the EO contains 22 electrocytes. It has a bilateral symmetry, as does the rest of the EO: on each side of the sagittal plane the electrocytes are aligned rostro-caudally and arranged in two columns (medial and lateral). Each column splits into two columns (dorsal and ventral) at its rostral end (Fig. 3A,B,D,E).

Each medial column consists of four electrocytes. Three are aligned rostro-caudally (medial electrocytes ME-1; ME-2; ME-3),

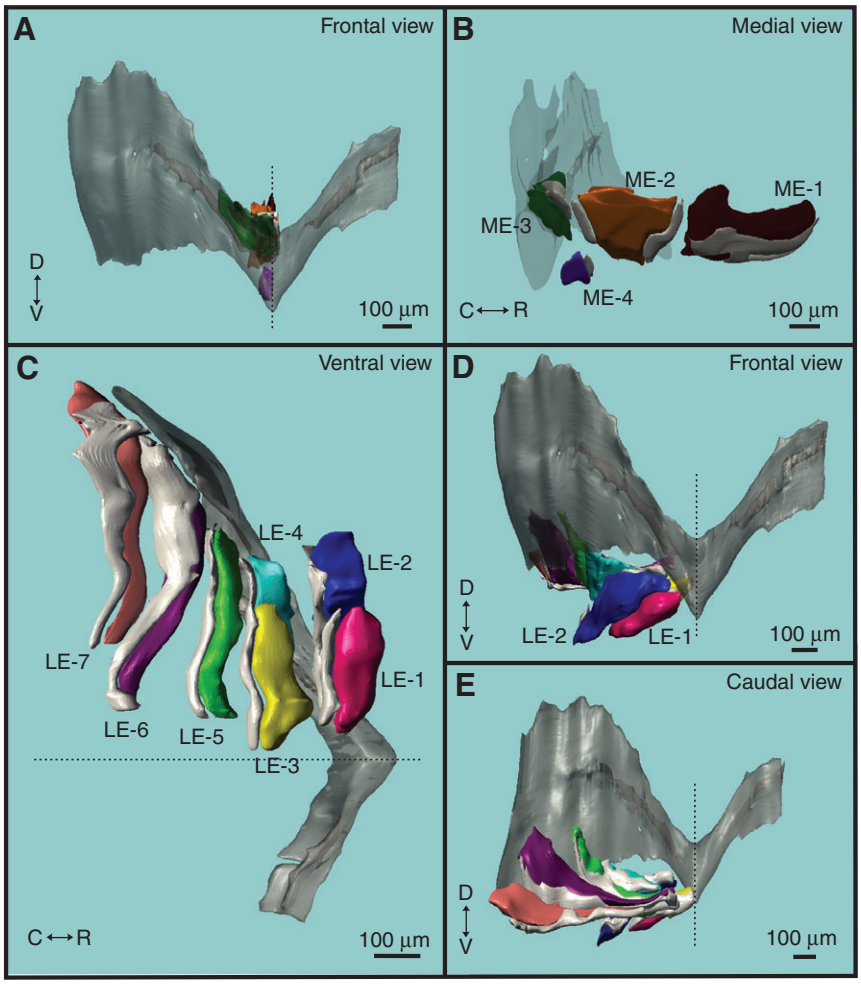

Fig. 3. Detailed organization and innervation pattern of the subopercular electric organ. Magnified views of the 3-D reconstruction showed in Fig. 2. The right medial column is shown from the frontal (A) and medial (B) view. (C,D,E) Ventral, frontal and caudal views, respectively, of the right lateral column. In all cases the cleithrum and the connective sheet that extends between the cleithrum and the operculum, separating the head from the rest of the body, are also shown. The whitish coloring indicates the innervated region of the electrocytes' surface. Four electrocytes form the medial column, three rostrocaudally aligned (medial electrocytes 1, 2 and 3: ME-1, ME-2 and ME-3, respectively), and a fourth one (ME-4), beneath ME-3 in the same parasagittal plane. ME-1 and ME-2 are elongated in the rostral-caudal and ventral-dorsal axis, and flattened in the lateral-medial axis. ME-1 is innervated at the ventral border and ventral side of its lateral and medial faces, whereas ME-2 is doubly innervated (the rostral and caudal borders). ME-3, with a ribbon-like shape, is mostly surrounded by the cleithrum bone (A,B). It is innervated on its caudal-dorsal face (B). ME-4 is cuboidal and is innervated at its dorsal-caudal face (A,B). The lateral column runs along an almost horizontal plane, parallel to the skin surface, with its head intruding below the connective sheet. It consists of seven ribbon-like electrocytes (L1 to L7 in C). Most of LE-1 and LE-2 are inside the head, LE-3 and LE4 are partially on both sides, and LE-5–LE-7 are caudal to the connective sheet (C). LE-1 to LE-4 are shorter, run perpendicular to the midline inside four rostral compartments (two dorsal and two ventral; C and D), and are innervated on their caudal borders (C). LE-5, which is of intermediate length, is innervated on its caudal border (C). The medial parts of LE-6 and LE-7 run diagonally with respect to the midline and are innervated on their caudal border and part of their ventral surface (C). The lateral half of these electrocytes bends up and hence the electromotor end terminals innervate their lateral surfaces (D,E).

and the fourth one (ME-4) lies beneath the ME-1 (Fig. 3A,B). ME-1 and ME-2 are flattened in the latero-medial axis and elongated in the rostro-caudal and ventro-dorsal axis to a lesser extent (Fig. 3B). ME-1 is innervated at the ventral side of the lateral and medial faces and its ventral border, whereas ME-2 is doubly innervated (nerve fibers end on both the rostral and the caudal borders; Fig. 3B). ME-3 is ribbon-like, elongated in the dorso-ventral axis and flattened in the rostro-caudal axis. It is mostly encased by the cleithra bones and follows its direction: the main axis of ME-3 runs lateral to medial and dorsal to ventral (Fig. 3A,B, Fig. 4A). It is innervated on its caudo-dorsal face (Fig. 3B, Fig. 4A). ME-4 is cubical and is innervated at its dorso-caudal face (Fig. 3B).

Each lateral column consists of seven rod-like electrocytes (lateral electrocytes, LE-1 to LE-7; Fig. 3C–E) elongated in the medio-lateral axis. This column follows an oblique course. The rostral region of the lateral column has four compartments, two ventro-medial and two dorso-lateral enclosing caudally innervated electrocytes LE-1 to LE-4 (Fig. 3C–E). The most rostral electrocytes, LE-1 (ventral) and LE-2 (dorsal) are short cylinders whose medial ends lie beneath the medial column. Each of the three caudal compartments encloses a single electrocyte, which are progressively longer and more lateral, from rostral to caudal (LE-5 to LE-7; Fig. 3C). These electrocytes bend up following the plane of the cleithrum-opercular ligament in such a way that the ventral face of the horizontal portion is continued by the lateral face of the ascending portion (Fig. 3D,E). The medial parts of the LE-5, LE-6 and LE-7 are horizontal, oriented either perpendicular (LE-5) or oblique (LE-6, LE-7) to the sagittal plane. They are innervated at the caudal (LE-5) or latero-caudal borders (LE-6, LE-7; Fig. 3C–E, Fig. 4B). This innervation extends on the ventro-lateral faces of the lateral ascending parts.

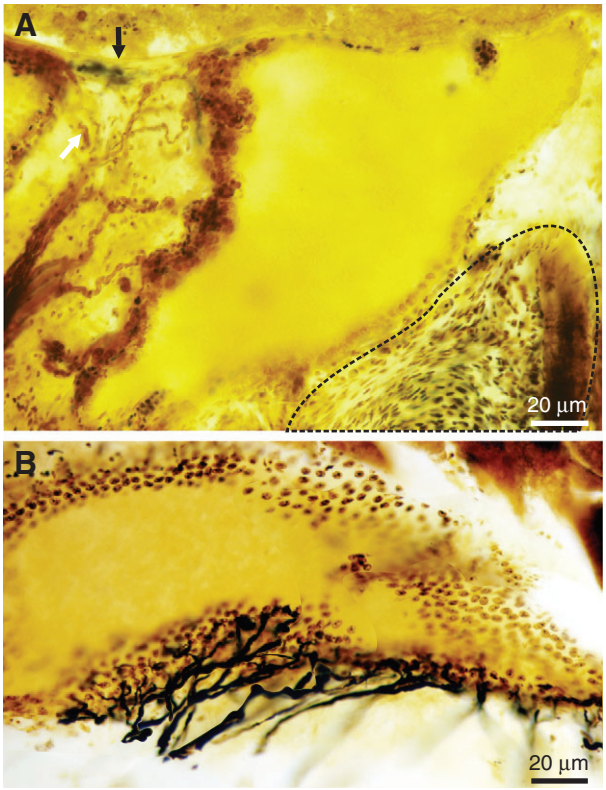

Fig. 4. Electrocyte innervation of the head portion of the EO. Examples of the electromotor end terminals contacting electrocytes of the medial (A) and lateral (B) columns as revealed by the silver impregnation technique. (A) Photomicrograph of a parasagittal section of the rostral and dorsal part of the medial column containing ECM1. Note the thin connective sheet that delimits the column (black arrow) where the whole of ECM1 and the rostral end of ECM2 are present. These electrocytes are separated by a gelatinous tissue traversed by a bunch of electromotor axons that reach and innervate the caudal face of ECM1. Some fibers (white arrow) course caudally to reach the rostral face of ECM2. Note the proximity of ECM1 to the cleithrum (dotted outline). (B) Collage of microphotographs of successive optical section in horizontal planes of an electrocyte of the lateral column and its innervating electromotor fibers reaching its caudal border where they ramify profusely.

The abdominal portion of the electric organ

The abdominal portion is included in the ventral abdominal wall (Fig. 5). It consists of four rostro-caudal tubes (two at each side of

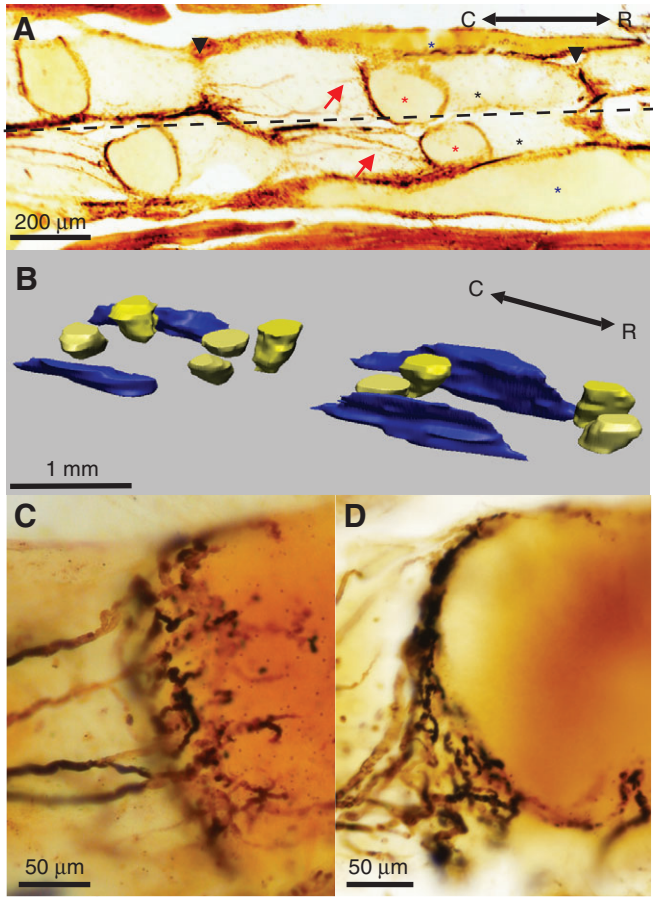

Fig. 5. The abdominal portion of the EO. (A) Microphotograph of a horizontal section of a Cajal and De Castro preparation showing its general organization: two columns on each side of the midline. The electrocytes of the medial and lateral columns are cuboidal (red asterisks) and fusiform (blue asterisks), respectively. The medial electrocytes are caudally innervated (red arrows) whereas lateral ones are innervated in their medial face and poles. Electrocytes occupy the medial region of compartments delimited by thin connective sheaths and filled with a gelatinous connective tissue. The black arrowheads indicate the septa between neighboring compartments of a medial column. (B) Computer 3-D reconstruction of the abdominal portion of the EO from serial horizontal sections as in A. Electrocytes are color-coded according to their type. Cuboidal electrocytes, aligned along medial columns, are innervated on their caudal faces (yellow). The lateral columns contain large fusiform electrocytes innervated on their medial faces and poles (blue). (C,D) Higher resolution micrographs show the innervation pattern of medial electrocytes in horizontal sections tangential to the surface (C) or at the middle (D).

the midline; Fig. 5A,B). The medial tubes enclose 'drum shaped', caudally innervated electrocytes (Fig. 5C,D), whereas the lateral columns have large, fusiform electrocytes having an extended innervation, covering their medial faces and their rostral and caudal poles. In 'photographic Cajal preparations', electrocyte density is about 1 mm^{-1} in the medial tubes and 0.5 mm^{-1} in the lateral ones (in a fish of 10 cm length). A flat nerve runs over the medial and lateral electrocyte tubes.

The main portion of the electric organ

The main portion of the EO is also located ventrally below the ventral muscle mass and comprises the EO portion occupying the most caudal five-sevenths of the body (from the origin of the anal fin to the tip of the tail). It consists of four tubes longitudinally aligned at each side of the midline (sections c to g in Fig. 1B, Fig. 6A). The dorsal tube (tube 1 in Fig. 6A) extends laterally between the ventral muscle mass and the fin muscle fibers. It contains fusiform-shaped electrocytes, flattened in the dorso-ventral direction. These electrocytes are innervated on their rostral and caudal poles, with some extension to the ventral aspect (Fig. 6B–D). The other tubes (tubes two to four in Fig. 6A) are aligned on a parasagittal plane with their medial aspects close to the midline. They contain caudally innervated, 'drum shaped' electrocytes of relatively smaller and more regular dimensions than the fusiform ones (Fig. 6E–G).

At the main portion of the EO (sections c–g, Fig. 1B) the distance between fusiform electrocytes was similar to the distances between drum-shaped electrocytes. Electrocyte density increased from 1 mm^{-1} at the rostral region of the main portion of the EO (about section c, Fig. 1B) to 4 mm^{-1} at the tail region (section f, Fig. 1B, 10 cm fish total length). The electrocytes of different tubes were out of register. Drum-type electrocytes of the three ventral tubes were organized resembling an orderly ladder with the dorsal electrocyte more caudal as evidenced in the parasagittal sections (Fig. 6E). At the tail region the dorso-lateral tubes approach the midline and the four tubes appear alike in transverse sections, except near the tip of the tail where only two or three tubes were found. Double innervation was found in the dorso-lateral tube up to the most caudal regions explored (about 95% of the fish body length). In the caudal quarter of the fish body, a thick nerve, running rostro-caudally above the dorsal tubes was evident (posterior electromotor nerve, sections f and g in Fig. 1B).

The electric organ discharge

The head to tail EOD associated field recorded in water (htEOD) of *G. coropinae* shows a complex pattern (Fig. 7, black and blue traces). This waveform showed striking differences with that of the EMF recorded in air (Fig. 7, red trace). These differences depended on the distance between the electrodes used for recording the htEOD. Since the waveform results from the overlapping of components generated at different regions of the fish body, it was necessary to take into account different types of recordings to identify the independent components of the EOD. Seven components were

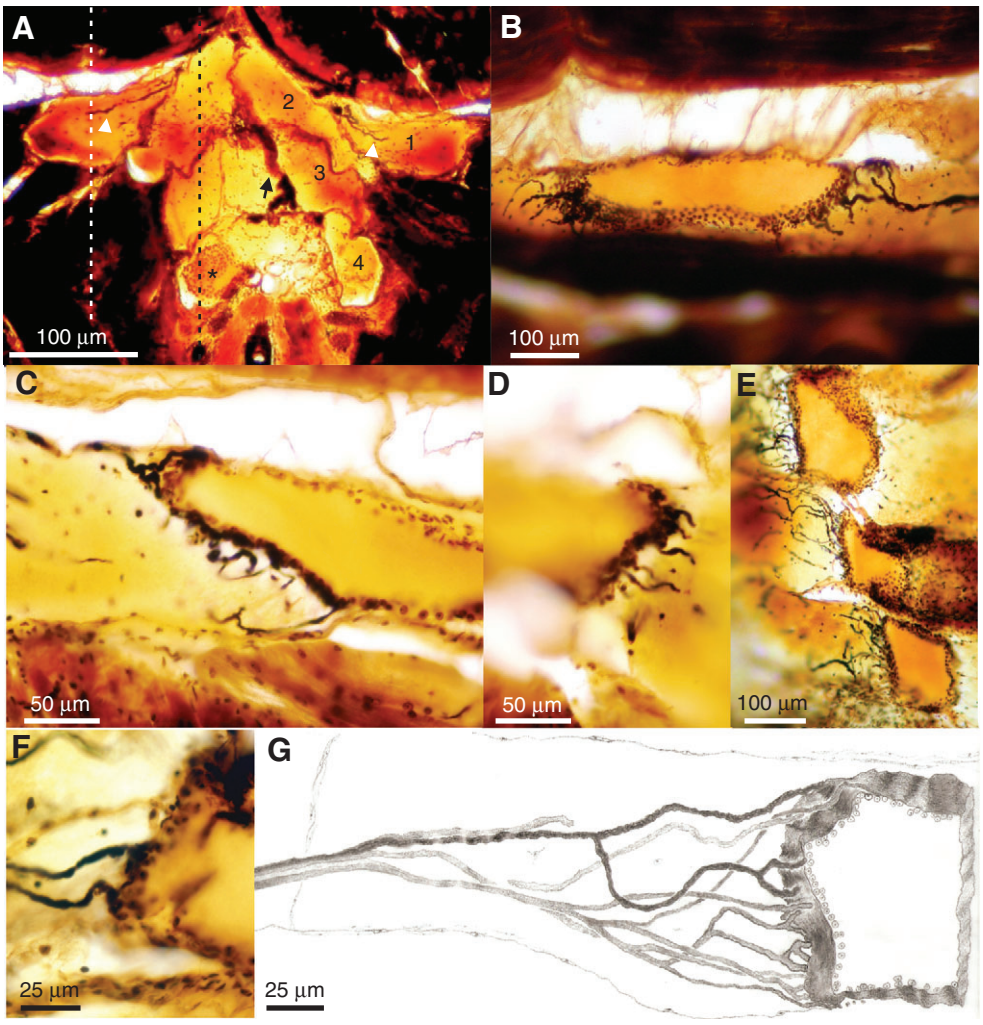

Fig. 6. The main portion of the EO. (A) Microphotograph of a frontal section of a Cajal and De Castro preparation. Note that the dorsal column (1) is elongated in the medial-lateral direction. It extends laterally between the ventral muscle mass and the fin muscles, partially overlapping the others at the medial border. Columns 2–4 lie on a parasagittal plane. In this section only on column 4 is an electrocyte visible (asterisk), whereas in some of the others, electromotor axons run within the jelly between electrocytes (arrowheads). A thick electromotor nerve (black arrow) runs along the sagittal plane. The white dashed line indicates the parasagittal plane corresponding to the microphotographs shown in B–D, and the black dashed line indicates the parasagittal plane corresponding to the microphotograph in E. (B–D) Micrographs of a parasagittal section, showing the innervation pattern of a fusiform electrocyte of column 1. Note that the terminal branches of the electromotor nerve innervate the lateral electrocytes on their poles and on adjacent ventral surfaces. (E) Low magnification micrograph of a parasagittal section showing the three ventral columns and the spatial relationship between cuboidal electrocytes of neighboring columns 2–4. (F,G) A micrograph and a camera lucida drawing of two cuboidal electrocytes and their caudal innervation.

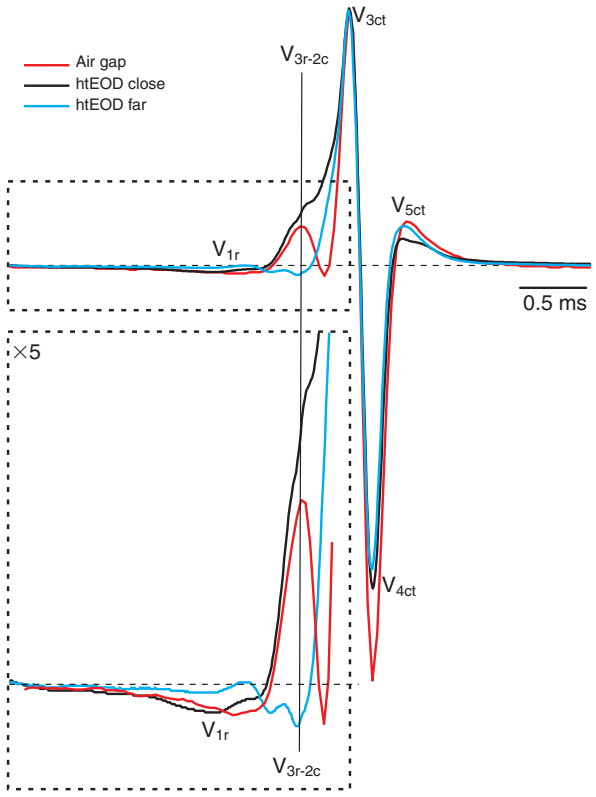

Fig. 7. The EOD waveform of *G. coropinae* depends on the recording conditions. The head to tail EOD (htEOD) of *G. coropinae* consists of six components (V_{1r}, V_{3r}, V_{2ct}, V_{3ct}, V_{4ct}, V_{5ct}). Classically the head to tail EOD has been used as a taxonomic tool for species identification. However, in the case of *G. coropinae* it shows important variations depending on the position of the recording electrode (near: black trace; far: blue trace) and also on load [compare waveforms obtained with the fish in the water (black trace) with the fish in the air (red trace)]. This indicates an important complexity at the earlier stages of the EOD. Recordings obtained with the air gap technique (red) show relatively larger and earlier wave components, in particular V_{3r}. As is better appreciated in the magnified inset (bottom boxed region), htEOD recordings in water, obtained between two electrodes placed on the main axis of the fish at 4 cm (black) and 16 cm (blue) from the skin surface show how V_{3r} is overcome by V_2 as the distance increases.

identified; six components originated in the EO. The seventh component, generated at the tail region, was a small ripple preceding the main peak, similar to that caused by the neural volley coordinating the EO in *G. omari* (Caputi and Aguilera, 1996). The components originating from the EO were named taking into account their order in the sequence (sub index 1–5), spatial origin (sub index r for rostral, c for central and t for caudal) and possible generation mechanisms (Rodríguez-Cattáneo et al., 2008): V_{1r} V_{3r}, V_{2c}, V_{3ct}, V_{4ct}, V_{5ct}. We will first give the evidence for their identification as individual components and then describe them as observed in the head to tail recordings.

In order to confirm the previously reported data, and to correlate the electrogeneration with the anatomical structure of the EO, we explored the spatial pattern of EMFs using the air gap technique (Caputi et al., 1993) and the near field in the vicinity of the fish body (Bennett and Grundfest, 1959). These procedures provided evidence for the sequence and spatial origin of the EOD components, allowing us to propose a generation mechanism. The air gap has some limitations because of two assumptions: (1) that the generators are aligned with the main axis of the fish, and (2) that the passive tissue surrounding the EO is nearly homogeneous and mostly resistive. In a ribbon-like small fish like *G. coropinae*, the drop of voltage recorded rostral to the anal fin depends on the circulation of current along complex paths as a result of the uneven resistance of different tissues (bone, abdominal cavity contents, swim bladder) and the potential short circuit caused by water flow through the gills.

Therefore, we recorded the region rostral to the anal fin (including the head and abdominal portions of the EO) as a single unit (two-sevenths of the fish length; Fig. 8A), and applied the near field potentials (Fig. 9) to refine the correlation with the anatomical findings.

The EOD waveform generated by the head and abdominal regions consists of a smooth negative wave (V_{1r}), a positive peak that was named V_{3r} because of its similarity and commonly proposed mechanism as the main peak (see Discussion), and a small negativity (V_{4r}; Fig. 8A, gap a). The perpendicular fields recorded every 2 mm, 2 mm away from the nearest point of the surface of the fish, showed a transition between the head and the abdominal regions for V_{1r} and V_{3r} (Fig. 9A). There is a rostral early sink (at the time of V_1) and a late source (at the time of V_{3r}) with the respective source (for V_{1r}) and sink (for V_{3r}) concentrated on the gill cleft (Fig. 9A,C,D). The reversal points are at the rostral limit of the cleft whereas the absolute maxima are near the caudal limit of the cleft. This suggests that the generators of V_1 and V_{3r} are situated at the level of the operculum, where we described the head portion of the EO. It also suggests that the gills are a preferred path for current circulation. During the rest of the EOD the head-abdominal region does not show reversal points in the transcutaneous currents suggesting that the generators are caudal to the anal fin (Fig. 9B,E–G).

The large sink observed at the opercular region begins a bit earlier than the source. This feature and the inward remnant (asterisk in Fig. 9D) caudal to the origin of the anal fin may indicate the presence of a concomitant, head negative generator located caudally, at the main portion of the EO (V_{2c}). This was confirmed by the air gap in which V_{2c} was present from the origin of the anal fin to the tail (b to f in Fig. 8A,B).

The rest of the fish body was explored in air gap conditions with a resolution of $1/7^{th}$ fish length (Fig. 8). In these regions, the EOD waveforms consisted of a negative-positive-negative-positive complex (V_{2345ct}). The peaks of these components increased from head to tail except for V_{2ct} that decayed at the most caudal region (Fig. 8B–E).

The electric organ discharge expressed as an electric field

The EOD is a potential effector act. It becomes a measurable fact, i.e. an electric field when the activation of electrogenic membranes makes currents flow against two kinds of loads: (1) internal, represented by the tissues of the fish and (2) external, represented by the surrounding water. *G. coropinae* provides us with an excellent example of how the EOD-associated electric field varies with position, distance and load.

The electric field recorded either near or far away from the fish's body is a weighted sum of the fields generated by the different sources already described. Since the different components above described are weighted in a dissimilar way, the field waveform is different when recorded with different electrode arrays (Bennett, 1971; Caputi, 1999). In order to call the reader's attention to the importance of this process, which is the focus of a full article to be published elsewhere, we first compare two kinds of head to tail measurements: simple air gap procedures (in which the weight of

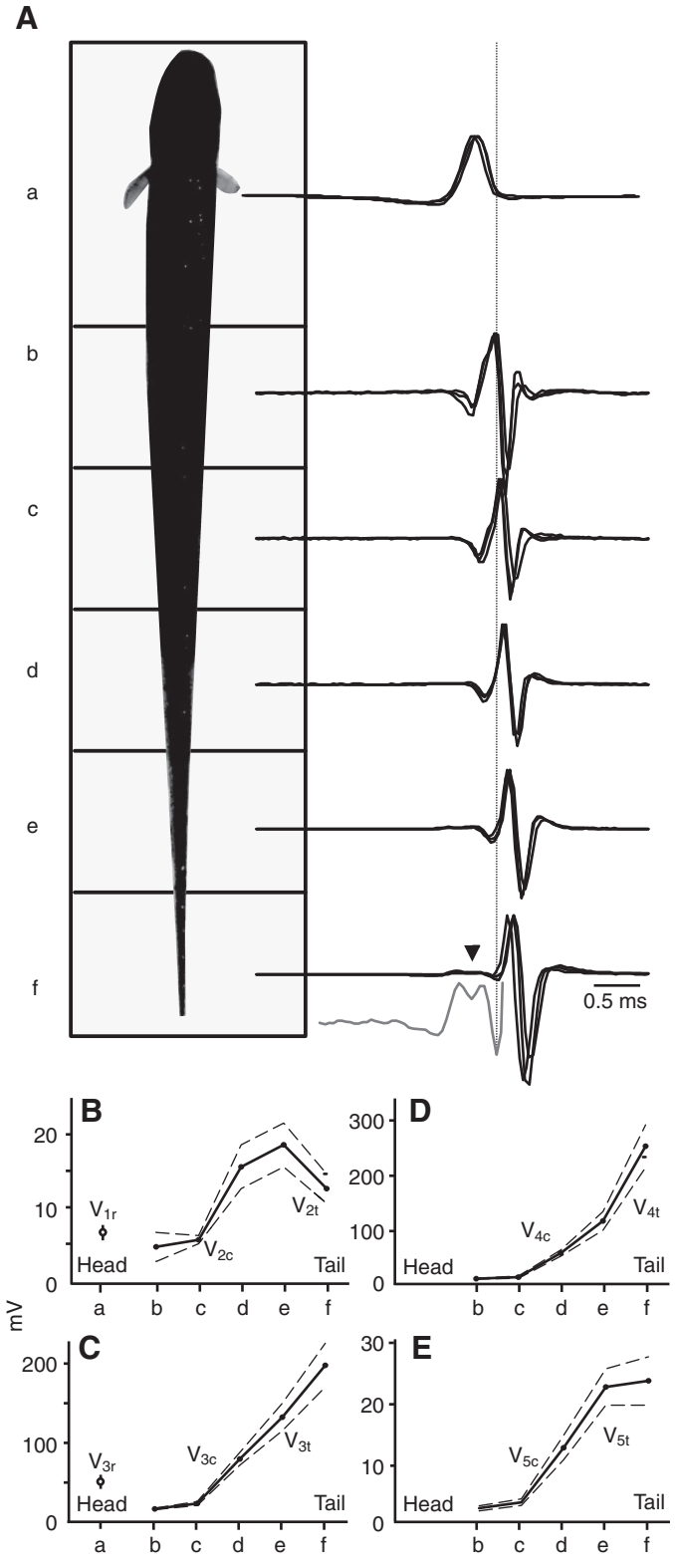

Fig. 8. The spatio-temporal pattern of activity as evidenced by the multiple air gap procedure. (A) The voltage drop generated by different portions of the fish's body was simultaneously recorded with the fish isolated in air. For the sake of clarity, data from only three fish are shown. The rostral portion (a) corresponds to two-sevenths of the fish length, and the others (b to f) to one-seventh each. For each gap between electrodes the normalized regional waveforms were aligned with respect to the main positive peak of the head to tail recordings of each fish. Note the fast progression of the activation along the fish body (approx. 500 m s^{-1}). The arrowhead in f indicates the neurally generated components preceding the activation of the tail region of the EO (one magnified example is shown as a gray trace). (B–E) Absolute amplitude of the waveform components of the EOD as a function of their origin along the EO (a to f as indicated in A, mean ± s.d., *N*=9). (B) V_{1r} and $V2_{ct}$; (C) V_{3r} and V_{3ct}; (D) $V4_{ct}$ (E) V_{5ct}.

the different components is determined only by the internal loads) and head to tail 'classical' recordings at different distances. Then, we compare the fields associated with homologous waves components generated by the subopercular (V_{3r}) and of the main EO (V_{3ct}).

In both cases, V_{1r} is the earliest and longest component lasting about 2 ms (Figs 7 and 10). It is a smooth head negative wave originated at the head (for this reason, we added the sub-index 'r', see above). However, the relative amplitude of this component was relatively large in the air gap and recordings obtained with the electrodes almost touching the head and tail (near field), whereas it was very much attenuated when the electrodes were placed at higher distances (far field).

Following V_{1r} there was a complex, the shape of which varied with load and distance (Figs 7, 10 and 11). As we show above, two differently located but simultaneously activated generators of opposite polarity explain such variability. The final output is the weighted sum of their influences on the environment. Depending on water conductivity and the relative position of the electrodes in relation to each of such sources, either a head positive or a head negative deflection can be recorded.

The electric field resulting from loading the fish's body with the surrounding water (30 μS cm^{-1}) illustrates how the earlier part or the EOD is important for generating localized fields whereas the later part generates a more global field. The field associated with the activation of rostral regions of the EO (V_{3r}, Fig. 9, Fig. 10, left vector map) concentrates around the head. At the same time the head negative field, possibly associated with the activation of rostral patches of the membrane of the dorso-lateral tube occurring from the abdominal region to the tail, generates another field (V_{2c}, Fig. 9, Fig. 10, left vector map). This causes the entrance of the current to the body through a single sink at the gill region and the rest of the current through two sources: one caudal (for V_{2c}) and other rostral (for V_{3r}). As observed in the figure, the distance between sink and source is longer for V_{2c} than for V_{3r}. As a consequence, locally near the fovea V_{3r} prevails, and far away (in the classical head to tail recordings made with an inter-electrode span of 48 cm) V_{2c} dominates.

The situation is rather different in the air gap where external currents are forced to flow longitudinally along the fish body closing the circuit between head and tail. The early positive peak (called V_{3r} because of the similar generation mechanism with the main peak V_{3ct}) stood out in air gap recordings (in which it completely dominated the negative one, V_2) indicating that caudal faces of large rostral electrocytes generate more current than the sparsely distributed doubly innervated electrocytes of tube 1. By contrast, V_2 overcame V_{3r} in the far field htEOD (Figs 9 and 10, blue traces, insets) probably because the far field generated by V_{3r} (having an equivalent shorter arm dipole) attenuates much more steeply than V_{2c} (having an equivalent longer arm dipole). Therefore, in the head to tail recordings (either in water or in air) we called this deflection $V_{3r\text{-}2c}$.

The htEOD ends with a sharp triphasic complex generated on the main region of the fish body, from the origin of the anal fin to

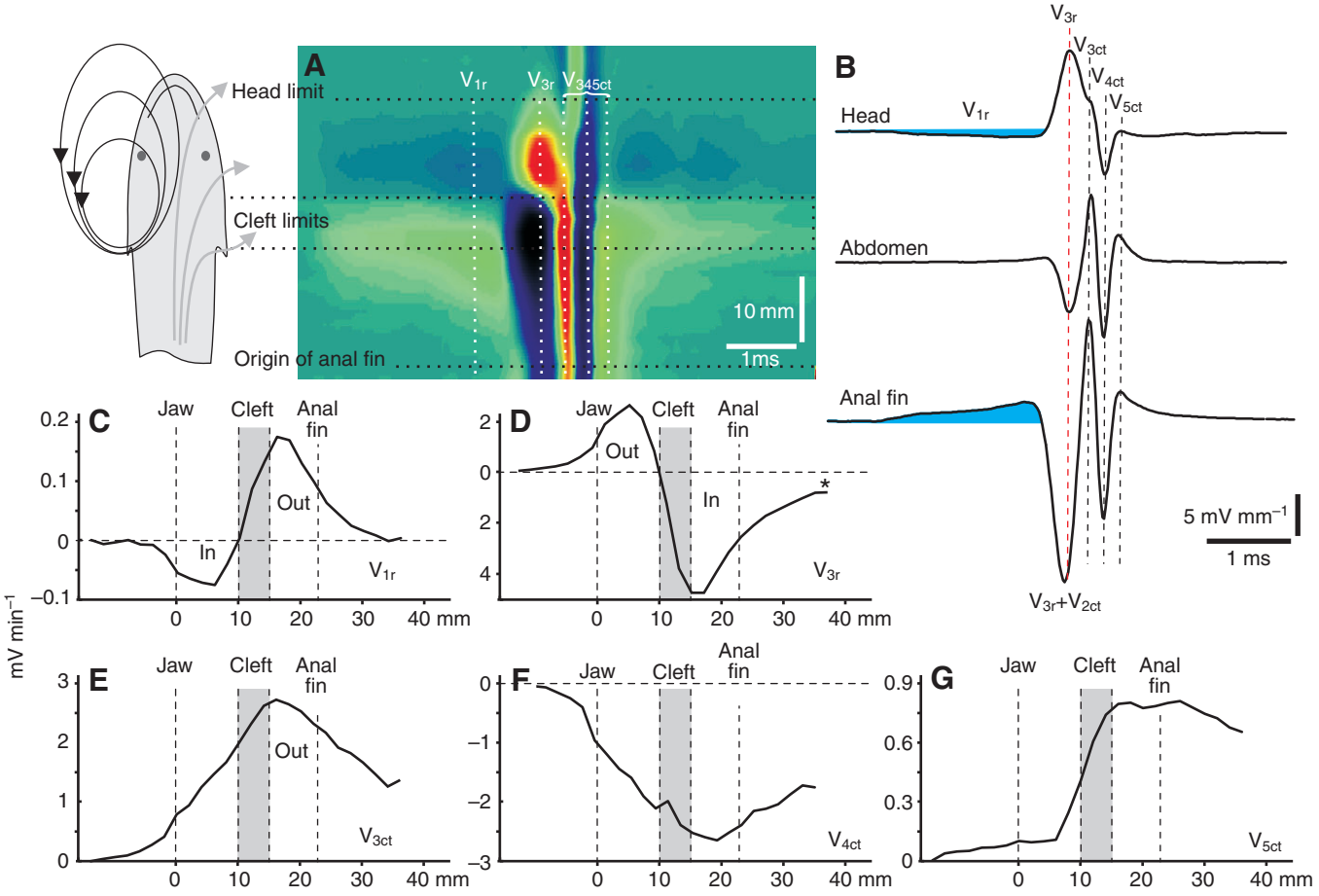

Fig. 9. Near field potentials along the rostral region of the fish body indicate the presence of a generator at the level of the operculum. (A) Color map showing the electric field perpendicular to the main axis of the fish body, recorded 2 mm away from the nearest point of the skin, as a function of the rostro-caudal position and time. The schema shows the rostral portion of the fish and exemplifies the flow of currents during V_{3r} (black) and V_{3ct} (gray). Color scale was non linearly adjusted [arctg (V)] to make the comparison between components easier. (B) Traces obtained at three different recording sites exemplify the inversion of V_{1r} (blue) and V_{3r} (red dotted line). (C–G) The amplitude of each of the components as a function of the recording position. There is a reversal point in the local field at about the limit of the head for V_{1r} and V_{3r} indicating a rostral source of these components (B–D). Conversely, the polarity of the other wave components did not change (B black dotted lines, E–G).

the tip of the tail (V_{345ct}), that was (as in the case of V_{1r}) present in both loading conditions (Figs 7, 10 and 11). The field resulting from the activation of the main region of the EO (V_{3ct}, Fig. 10, right vector map) is characterized by a very long distance between sink and sources in all components. Consequently the influence of the main region of the EO extends far away, dominating the far field.

Head to tail air gap recordings also allowed us to study the characteristics of the sources giving origin to each of the main components. V_{1r} was not explored because of its low amplitude relative to noise when the loading resistance was decreased. V_{3r} and V_{2ct} were inextricable because of their simultaneity. Therefore we explored the voltage *versus* current relationship at the peaks of the positive-negative-positive complex. We found two kinds of characteristic curves: linear and non-linear. Voltage was a linear decreasing function of the current for $V_{3r\text{-}2c}$ and V_{3ct}, as occurs in neurally driven components. The slopes of the fitting lines for $V_{3r\text{-}2c}$ were always significantly steeper than the fitted slopes for V_{3ct} (Fig. 11B,C) indicating the difference in the internal resistance for their generators. Contrasting with the sharp positive peaks, V_{4ct} slightly departed from linearity when load resistance increased (Fig. 11D) and the last positive wave (V_{5ct}) showed a clear convex relationship (Fig. 11E). This indicates that the electromotive force depends on the load in a non linear way. Accordingly with a non neural activation of the electrocyte electrogenic membrane, the ratios V_4/V_3 and V_5/V_4 increased with the current generated, respectively, by V_{3ct} and V_{4ct} (Fig. 11F–G) (Rodríguez-Cattáneo et al., 2008).

DISCUSSION

Three main findings characterize the EO and EOD organization of *G. coropinae* described here in relation to the EO and EOD of other gymnotids.

The first finding is that the EO extends into the head region where it generates a waveform characterized by triphasic sequence (slow negative wave – broad positive peak – small negative peak; V_{134r} complex; Fig. 8), very similar to that observed in *G. omari*. This waveform dominates the local electric field in the surroundings of the head (Fig. 9). However, the structure and innervation pattern of the EO in this region suggest that this negative–positive–negative discharge is not generated by exactly the same mechanisms as in *G. omari* [as described by Lorenzo et al. (Lorenzo et al., 1988)].

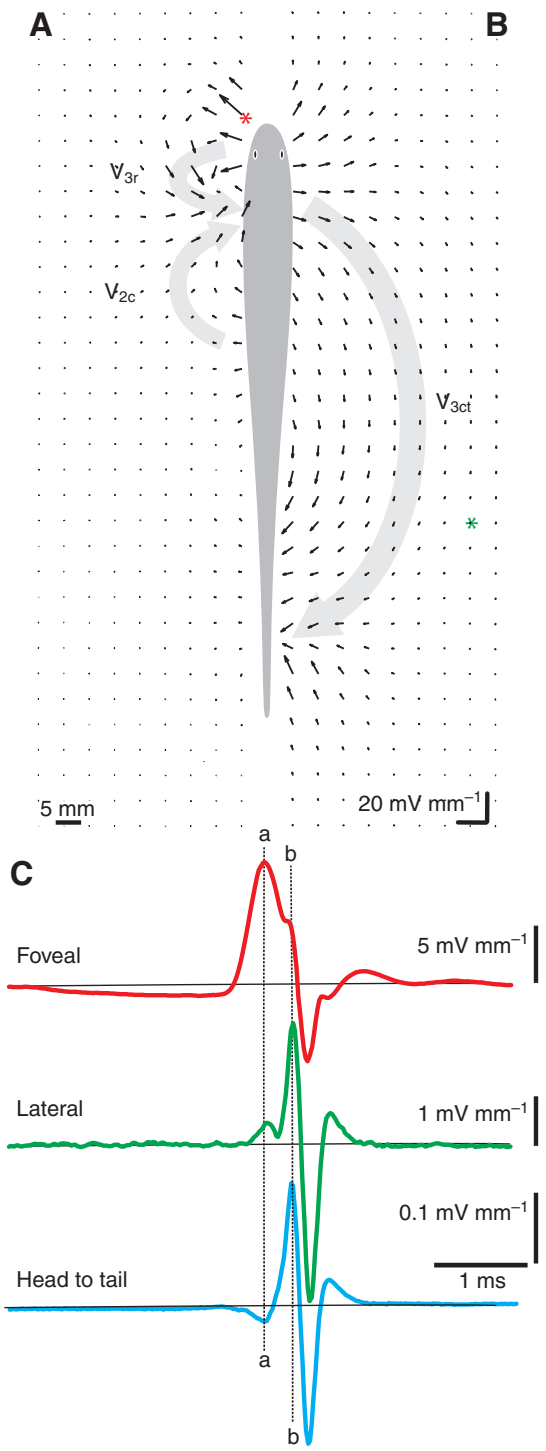

Fig. 10. Field potentials at two different times of the EOD. 'Vector maps' were constructed by plotting the field vectors at the intersection of perpendicular and parasagittal lines, 5 mm apart, on the horizontal plane passing through the fish's main longitudinal axis. Raw data were interpolated to duplicate the number of vectors in each row and column. (A) 'Vector map' of the field at the time of V_{3r} and V_{2c} (line labeled as A over the traces in C). Note that there is a single sink flanked by two sources (large gray shaded arrows). (B) 'Vector map' of the field at the time of V_{3ct} (line labeled as B over the traces in C). Note the larger distance between the sink and the source (large gray shaded arrow). (C) Selected recordings of field as a function of time taken near the fovea (red asterisk and trace) and lateral to the fish (green asterisk and trace) are compared with the head to tail EOD (blue trace).

Although the local electrosensory carrier around the head region is mainly generated by the abdominal portion of the EO in *G. omari*, it is mostly generated by the head portion of the EO in *G. coropinae*. In fact, in this species, the electrocytes that putatively generate the slow negative component are the two pairs of doubly innervated electrocytes of the head portion of the EO and perhaps the fusiform, medially innervated electrocytes of the abdominal wall. In addition, the broad head positive peak generated at the head region must have its main origin in the activation of the latero-caudal faces of the seven electrocytes of the lateral tubes of the head portion of the EO. The laterally innervated face of LE-5 to LE-7 facilitates the circulation of currents from lateral to medial at the level of the opercular cleft. These currents are then funneled rostrally by the portion of the lateral tubes running below the cleithrum aponeurotic sheath. This causes a more localized field around the head, dominated by relatively low frequency components. The ventral extension of the innervation may be responsible for a vertical component of the field that we did not explore in this study. Contrasting with this relatively strong generator at the head, the abdominal portion of the EO generates a relatively weak EOD. This is in agreement with the presence of the small and sparse cuboidal electrocytes in the medial tube. However, it is difficult at this point to explain the role of the large lateral fusiform abdominal electrocytes, as they have an extended innervated inner face.

In spite of the unknowns still remaining, we may conclude that these rostrally generated components of the discharge appear not to be evolutionarily homologous to those generated by *G. omari* but rather to be homoplastic. In fact, the near field stimulating the foveae of *G. coropinae*, in the present study, *G. omari* (Castelló et al., 2000) and other *Gymnotus* (A.A.C., P.A.A., A.C.P. and A.R.-C., unpublished) are very similar traits implemented by very different cellular mechanisms.

The second finding is that the EO in the central and tail regions of the body is more or less homogeneous in structure and innervation pattern and this is reflected in the regional EOD waveforms. A single dorsal tube containing doubly innervated fusiform electrocytes appears to be the candidate for generating V_{2ct}, whereas the other three tubes, bearing caudally mono innervated electrocytes, appear to be the best candidates for generating the rest of the complex (V_{345ct}). As expected from this hypothesis, the peak amplitude of the complex V_{345ct} monotonically increases with electrocyte density. Nevertheless, we still are unable to explain the decay in amplitude of V_{2ct} at the caudal end. Owing to the over impregnation of the caudal 5% of the EO we could not estimate the relative density of fusiform and cuboidal electrocytes within this region.

Following the most parsimonious reasoning (Bennett, 1971; Caputi, 1999), the rostro-ventral innervated faces of the fusiform electrocytes of the dorso-lateral tube of the main portion of the EO appear to be the best candidates to generate V_{2ct}. Because this component initiates the regional EOD it should probably be neurally driven and according to Pacini's rule ("the negativity indicates the innervation site") it should be generated by a rostrally innervated electrocyte membrane.

The caudally innervated cuboidal electrocytes of the three ventral tubes of the main portion of the EO are similar to those of other gymnotids. This plesiomorphic structure generates the main positive peak (V_{3ct}), the constant component of the EOD waveforms of *Gymnotus* (Albert and Crampton, 2005). The responsiveness of these cuboidal electrocytes in *G. coropinae* appears to be different from those in other species (*G. omari*, *Brachyhypopomus pinnicaudatus*). In *G. coropinae*, V_{3ct} shows a voltage *versus* current linear relationship (range for r^2=0.987–0.998, P<0.001) whereas V_{4ct} and V_{5ct} showed

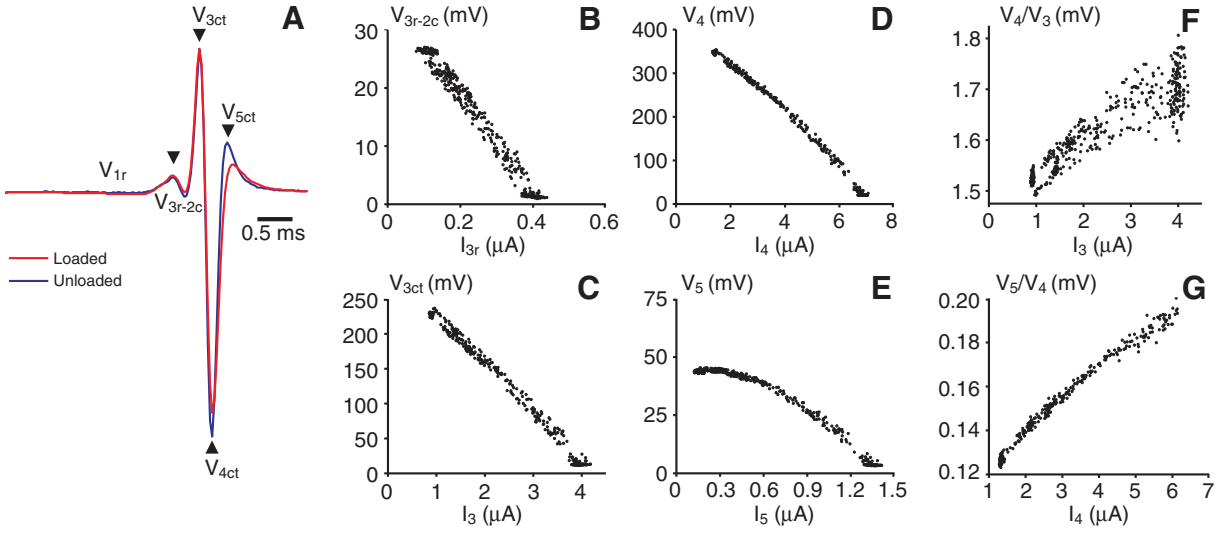

Fig. 11. Characteristic curves of the fish's body equivalent sources. (A) The normalized htEOD waveform obtained in the single air gap with a loading resistance of 2 MΩ (blue trace) and 15 kΩ (red trace) varies with load, indicating a non linear voltage–current relationship of some wave components. In the case of both V_{3r} and V_{3ct} (B and C) data are well fitted by lines (V_{3r}: r^2=0.978, P<0.0001, N=439; V_{3ct}: r^2=0.99, P<0.0001, N=439). The ordinate crossing value is a good index of electromotive force whereas the slope is an index of internal resistance. Note the difference in slope (V_{3r}: –0.085±0.001; V_{3ct}: –0.07±0.007) suggesting a drop in resistance caused by the activation of the main portion of the EO. In the case of both V_4 and V_5 (D and E), the relationship departs from linearity, suggesting a load-dependent recruitment of the electrogenic membranes. This is compatible with the increase of the ratios V_4/V_3 (F) and V_5/V_4 (G) as a function of the currents generating the preceding peak.

a non linear characteristic curve, indicating a load-dependent electromotive force (Fig. 11F,G). The shape of the curves, the dependence of the ratio V_4/V_3 on the current flowing during V_3, and the dependence of the ratio V_5/V_4 on the current flowing during V_4 are also compatible with the hypothesis that V_{345ct} is generated by the small, cuboidal, caudally innervated very excitable electrocytes. As occurs in most pulse gymnotids, current generating V_3 may flow rostrally, activating the rostral faces and generating V_4. In turn, V_4-associated current may activate again, but partially, the caudal faces generating V_5. Notably, the larger amplitude of V_5 for higher currents associated with V_4 may correspond to the presence of a very brief refractory period, suggesting a fast kinetics of the sodium channels in this species. In addition, the internal resistance measured for V_{3r} was systematically and significantly larger than for V_{3ct} (Fig. 10B,C). This rostro-caudal decay in global resistance may also indicate a large reduction in the EO longitudinal resistance, in spite of the small ratio between the electrogenic and non-electrogenic surfaces in the cross-section of the fish.

The third finding is the matching of the neurally determined interval (V_{2ct}–V_{3ct}) with the peripherally determined intervals (V_{3ct}–V_{4ct} and V_{4ct}–V_{5ct}), contributing to the V_{2345} complex. Gymnotid waveforms, which different from those of mormyrids in which EOD waveforms are mainly dependent on the shape and channel repertoires of the electrocytes, also depend on the neural control of the activation of electrocyte membrane patches (Hopkins, 1995; Aguilera, 1997). Matching between the intervals depending on the neural pattern of activation and the pattern resulting from electrocyte responsiveness may sharpen the power spectra of the species-specific EODs. This finding is not exclusive of *G. coropinae* as shown in Fig. 12, where the intervals between components of the EOD of three species are compared. This may indicate a co-evolution of the neural mechanisms of coordination and the intrinsic properties of the electrocytes of the main region of the body and is consistent with the presence of electroreceptors tuned to the species frequency power spectra (Bastian, 1977; Watson and Bastian, 1979).

This finding is also consistent with a modular organization of the EOD discharge. The modules are sequentially recruited from head to tail following a very fast sweep at an apparent speed of 500 m s^{-1}. This apparent speed is similar to that observed in other species: *G. omari* (Caputi et al., 1989; Caputi et al., 1993), *R. rostratus* (Caputi et al., 1994) and *B. pinnicaudatus* (Caputi et al., 1998) in which a neural network coordinates the progression of activation from rostral

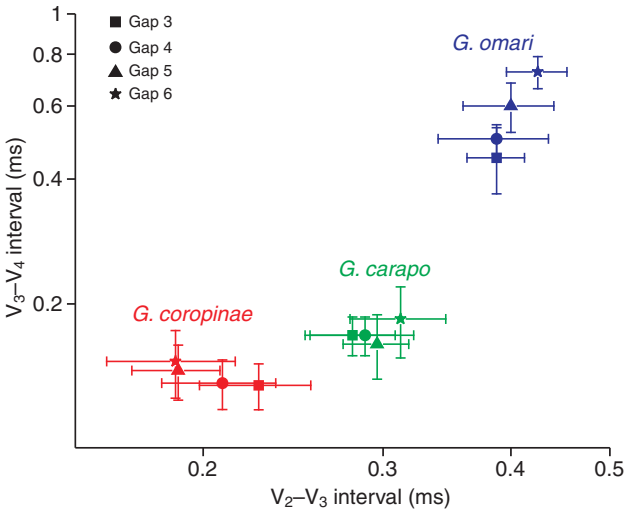

Fig. 12. Co-evolution of neurally and peripherally determined mechanisms of EO activation. Peripherally determined intervals (between V_3 and V_4) and neurally determined intervals (between V_2 and V_3) were measured for the signals obtained from gaps b to e defined in Fig. 8 in three species and represented in a Cartesian plot. Each symbol corresponds to a gap and each color to a species (mean ± s.d.). Data from A.R.-C. MSc thesis work (unpublished). *G. carapo* (N=5) and *G. omari* (N=4). Data from each species are grouped in a well-separated cluster from the other species.

to caudal regions of the EO (Caputi and Aguilera, 1996), and the sequence of the waves generated in each region of the EO (Aguilera, 1997; Caputi, 1999).

Interestingly, the rostrally generated complex (V_{134r}) preceded the centro-caudal complex (V_{2345ct}) in such a way that V_{3r} and V_{2ct} are isochronous. This, in addition to the large attenuation of V_{1r} with distance, causes large differences between the EOD-associated fields recorded in the surroundings of the fish's fovea and those recorded far away. This suggests that, whereas the broad head and abdominally generated V_{134r} sequence is more important for active electric exploration of the near environment, V_{2345ct} is more important for communication.

The short period between the wave components of the complex generated at the main portion of the EO appear to be an adaptation for shifting up the peak power frequency in the far field. This contrasts with the broader discharge occurring earlier at the head region. This broader waveform is similar to that observed in other *Gymnotus*, but it is probably based on different, homoplastic, electrogenic mechanisms. The rostral near field is mainly generated by a few electrocytes with very large electrogenic surfaces, and thus with a very low resistance. Thus, this voltage source may be likened to a dipole with a short arm. This field receives a small contribution from the larger population of smaller electrocytes with higher internal resistance located at the main portion of the EO. This extended population behaves as a current source that is the only significant contributor to the 'far field'. In fact, far away from the body the field can be closely described by the field of a single dipole having a long arm (Knudsen, 1975). The length of the dipole's arm depends on the length of the main portion of the EO and is expanded by the rostral funneling of the caudally generated currents due to the caudal tapering of the fish's body. The strength of the caudal dipole is much larger than that of the rostral one due to the increase in electrocyte density at the caudal regions. All these reasons explain the relatively larger weight of rostrally generated components around the head region and the relative larger weight of the caudally generated components at the far field.

In conclusion, the anatomical and functional observations here presented indicate that *G. coropinae* possesses a single EO with a dual function. Although the rostral regions of the organ generate a complex characterized by a smooth negative wave followed by a broad spike, the main portion of the EO generates a fast, tetraphasic complex. The 'perifoveal near field' is dominated by the contribution of the rostral portion of the EO and the 'far field' is dominated by the contribution of the caudal portion. The resultant differences in the power spectra of the near and far fields are more marked than in other gymnotids and might be more easily discriminated by differently tuned electroreceptor populations. Therefore, *G. coropinae* provides an excellent example of how near and far fields can support a different function: the rostral generated field is a better stimulus for the fish's own fovea, but it is more attenuated than the body-tail-generated field, which better serves a communication function (Aguilera et al., 2001; Caputi et al., 2002).

This study was partially funded by a NSF grant 0614334, Urufarma grant, and PEDECIBA Uruguay. Authorship: anatomy M.E.C., L.I., A.A.C.; physiology: A.R.C., P.A.A., A.C.P., A.A.C. First draft: A.A.C., M.E.C. and P.A.A.

REFERENCES

Aguilera, P. (1997). *Mecanismos espinales de coordinación de la descarga del órgano electrogénico en* Gymnotus carapo*: un estudio realizado mediante potenciales de campo.* MSc Thesis, PEDECIBA-Facultad de Ciencias, Universidad de la República, Uraguay.

Aguilera, P. A., Castelló, M. E. and Caputi, A. A. (2001). Electroreception in *Gymnotus carapo*: differences between self-generated and conspecific-generated signal carriers. *J. Exp. Biol.* **204**, 185-198.

Albert, J. S. and Crampton, W. (2005). Diversity and phylogeny of neotropical electric fishes (Gymnotiformes). In *Electroreception* (ed. T. H. Bullock, C. D. Hopkins, A. N. Popper and R. R. Fay), pp. 360-409. New York: Springer.

Bacelo, J., Engelmann, J., Hollmann, M., von der Emde, G. and Grant, K. (2008). Functional foveae in an electrosensory system. *J. Comp. Neurol.* **511**, 342-359.

Bastian, J. (1977). Variations in the frequency response of electroreceptors dependent on receptor location in weakly electric fish (Gymnotoidei) with a pulse discharge. *J. Comp. Physiol. A* **121**, 53-64.

Bell, C. C., Bradbury, J. and Russell, C. J. (1976). The electric organ of a Mormyrid as a current and voltage source. *J. Comp. Physiol. A* **110**, 65-88.

Bennett, M. V. L. (1971). Electric organs. In *Fish Physiology*, vol. 5 (ed. W. S. Hoar and D. J. Randall), pp. 347-491. London: Academic Press.

Bennett, M. V. L. and Grundfest, H. (1959). Electrophysiology of electric organ in *Gymnotus carapo*. *J. Gen. Physiol.* **42**, 1067-1104.

Caputi, A. A. (1999). The electric organ discharge of pulse gymnotiforms: the transformation of a simple impulse into a complex spatiotemporal electromotor pattern. *J. Exp. Biol.* **202**, 1229-1241.

Caputi, A. and Aguilera, P. (1996). A field potential analysis of the electromotor system in *Gymnotus carapo*. *J. Comp. Physiol. A* **179**, 827-835.

Caputi, A. A. and Budelli, R. (2006). Peripheral electric imaging in freshwater electric fish. *J. Comp. Physiol. A* **192**, 587-600.

Caputi, A., Macadar, O. and Trujillo-Cenóz, O. (1989). Waveform generation of the electric organ discharge in Gymnotus carapo. III. Analysis of the fish body as an electric source. *J. Comp. Physiol. A* **165**, 361-370.

Caputi, A., Silva, A. and Macadar, O. (1993). Electric organ activation in *Gymnotus carapo*: spinal origin and peripheral mechanisms. *J. Comp. Physiol. A* **173**, 227-232.

Caputi, A., Macadar, O. and Trujillo-Cenóz, O. (1994). Waveform generation in *Rhamphichthys rostratus* (L.) (Teleostei, Gymnotiformes): the electric organ and its spatiotemporal activation pattern. *J. Comp. Physiol. A* **174**, 633-642.

Caputi, A., Silva, A. and Macadar, O. (1998). The effect of environmental variables on waveform generation in *Brachyhypopomus pinnicaudatus*. *Brain Behav. Evol.* **52**, 148-158.

Caputi, A. A., Castelló, M. E., Aguilera, P. and Trujillo-Cenóz, O. (2002). Peripheral aspects of electrolocation and electrocommunication in *Gymnotus carapo*, *J. Physiol. Paris* **96**, 493-505.

Caputi, A. A., Carlson, B. A. and Macadar, O. (2005). The electric organs and their control. In *Electroreception* (ed. T. H. Bullock, C. D. Hopkins, A. N. Popper and R. R. Fay), pp. 410-452. New York: Springer.

Castelló, M. E., Aguilera, P. A. and Caputi, A. A. (2000). Electroreception in *Gymnotus carapo*: pre-receptor processing and the distribution of electroreceptor types. *J. Exp. Biol.* **203**, 3279-3287.

Couceiro, A. and De Almeida, D. F. (1961). The electrogenic tissue of some gymnotidae. In *Bioelectrogenesis: A Comparative Survey of its Mechanisms With Particular Emphasis on Electric Fishes* (ed. C. Chagas and A. Paes de Carvalho), pp. 3-19. Amsterdam: Elsevier.

Cox, R. T. and Coates, C. W. (1938). Electrical characteristics of the electric tissue of the electric eel, *Electrophorus electricus* (Linnaeus). *Zoologica* **23**, 203-212.

Crampton, W. G. R. and Albert, J. S. (2003). Redescription of *Gymnotus coropinae* (Gymnotiformes, Gymnotidae), an often misidentified species of Neotropical electric fish, with notes on natural history and electric signals. *Zootaxa* **348**, 1-20.

Darwin, C. (1866). *On the Origin of Species*, 4th edn. London: John Murray.

Hoedeman, J. J. (1962). Notes on the ichthyology of Surinam and other Guianas. 9. New records of gymnotid fishes. *Bull. Aquat. Biol.* **3**, 53-60.

Hopkins, C. D. (1976). Stimulus filtering and electroreception: tuberous electroreceptors in three species of Gymnotoid fish. *J. Comp. Physiol. A* **111**, 171-207.

Hopkins, C. D. (1995). Convergent design for electrogenesis and electroreception. *Curr. Opin. Neurobiol.* **5**, 769-777.

Hopkins, C. D. and Bass, A. H. (1981). Temporal coding of species recognition signals in an electric fish. *Science* **212**, 85-87.

Hopkins, C. D., Comfort, N. C., Bastian, J. and Bass, A. H. (1990). Functional analysis of sexual dimorfism in an electric fish, *Hypopomus pinnicaudatus* order Gymnotiformes. *Brain Behav. Evol.* **35**, 350-367.

Knudsen, E. I. (1975). Spatial aspects of the electric fields generated by weakly electric fish. *J. Comp. Physiol. A* **99**, 103-118.

Lissmann, H. W. (1951). Continuous electrical signals from the tail of a fish, *Gymnarchus niloticus* Cuv. *Nature* **167**, 201-202.

Lissmann, H. W. (1958). On the function and evolution of electric organ in fish. *J. Exp. Biol.* **35**, 156-191.

Lissmann, H. W. and Machin, K. E. (1958). The mechanism of object location in *Gymnarchus niloticus* and similar fish, *J. Exp. Biol.* **35**, 451-486.

Lorenzo, D., Velluti, J. C. and Macadar, O. (1988). Electrophysiological properties of abdominal electrocytes in the weakly electric fish *Gymnotus carapo*. *J. Comp. Physiol. A* **162**, 141-144.

McGregor, P. K. and Westby, G. W. M. (1992). Discrimination of individually characteristic electric organ discharges by a weakly electric Fish. *Anim. Behav.* **43**, 977-986.

Mohres, F. P. (1957). Elektrische Entladungen im Dienste der Revierabgrenzung bel Fischen. *Naturwissenschaften* **44**, 431-432.

Pereira, A. C., Rodríguez-Cattaneo, A., Castelló, M. E. and Caputi, A. A. (2007). Post-natal development of the electromotor system in a pulse gymnotid electric fish. *J. Exp. Biol.* **210**, 800-814.

Pusch, R., von der Emde, G., Hollmann, M., Bacelo, J., Nobel, S., Grant, K. and Engelmann, J. (2008). Active sensing in a mormyrid fish: electric images and peripheral modifications of the signal carrier give evidence of dual foveation *J. Exp. Biol.* **211**, 921-934.

Ramón y Cajal, S. and De Castro, F. (1933). *Elementos de técnica micrográfica del sistema nervioso.* Buenos Aires: Salvat Editores.
Rodríguez-Cattáneo, A., Pereira, A. C., Aguilera, P. A., Crampton, W. G. R. and Caputi, A. A. (2008). Species-specific diversity of a fixed motor pattern: the electric organ discharge of *gymnotus. PLoS ONE* **3**, e2038.
Sierra, F. (2007). *El Órgano Eléctrico de* Gymnotus*: mecanismos iónicos responsables de su descarga.* PhD Thesis, PEDECIBA-Facultad de Ciencias, Universidad de la República, Uraguay.
Silva, A., Quintana, L., Ardanaz, J. L. and Macadar, O. (2002). Environmental and hormonal influences upon EOD waveform in gymnotiform pulse fish. *J. Physiol. Paris* **96**, 473-484.
Stoddard, P. K. (1999). Predation enhances complexity in the evolution of electric fish signals. *Nature* **400**, 254-256.
Stoddard, P. K. (2006). Plasticity of the electric organ discharge waveform: contexts, mechanisms, and implications for electrocommunication. In *Communication in Fishes* (ed. F. Ladich, S. P. Collin, P. Moller and B. G. Kapoor), pp. 623-646. Enfield: Science Publisher.
Szabo, T. (1961). Les organes électriques de *Gymnotus carapo. Proc. K. Ned. Akad. Wet. C* **64**, 584-586.
Trujillo-Cenóz, O. and Echagüe, J. A. (1989). Waveform generation of the electric organ discharge in *Gymnotus carapo*. I. Morphology and innervation of the electric organ. *J. Comp. Physiol. A* **165**, 343-351.
Trujillo-Cenóz, O., Echagüe, J. A. and Macadar, O. (1984). Innervation pattern and electric organ discharge waveform in *Gymnotus carapo* teleostei Gymnotiformes. *J. Neurobiol.* **15**, 273-281.
Von der Emde, G. and Schwartz, S. (1999). Imaging of Objects through active electrolocation in *Gnathonemus petersii. J. Physiol. Paris* **96**, 431-444.
Watson, D. and Bastian, J. (1979). Frequency response characteristics of the electroreceptors in the weakly electric fish, *Gymnotus carapo. J. Comp. Physiol.* **134**, 191-202.